Appl. Sci. Converg. Technol. 27(4): 65-69 (2018)
https://doi.org/10.5757/ASCT.2018.27.4.65

Research Paper

Characteristics of Critical Pressure for a Beam Shape of the Anode Type Ion Beam Source

Yunsung Huh[a,*], Yunseok Hwang[a], and Jeha Kim[b,*]
[a]*R&D Center, Finesolution Co., Ltd., Suwon 16642, Korea*
[b]*Department of Energy Convergence Engineering, Cheongju University, Cheongju 28503, Korea*

Received June 8, 2018; revised June 25, 2018; accepted July 9, 2018

Abstract We studied the critical pressure characteristics of an anode type ion beam source driven by both charge repulsion and diffusion mechanism. The critical pressure P_{crit} of the diffusion type ion beam source was linearly decreased from 2.5 mTorr to 0.5 mTorr when the gas injection was varied in 3~10 sccm, while the P_{crit} of the charge repulsion ion beam source was remained at 3.5 mTorr. At the gas injection of 10 sccm, the range of having normal beam shape in the charge repulsion ion beam source was about 6.4 times wider than that in the diffusion type ion beam source. An impurity of Fe 2p (KE = 776.68 eV) of 12.88 at. % was observed from the glass surface treated with the abnormal beam of the charge repulsion type ion beam source. The body temperature of the diffusion type ion beam source was observed to increase rapidly at the rate of 1.9°C/min for 30 minutes and to vary slowly at the rate of 0.1°C/min for 200 minutes for an abnormal beam and normal beam, respectively.

Keywords: Anode type ion beam source, Critical pressure, Diffusion mechanism, Charge repulsion mechanism, Ion beam shape

I. Introduction

At present, the use of thin film process in various industrial fields such as semiconductors, displays, automobiles, and building exterior materials is gradually increased in association with the added functionalities. In general, the heat treatment in most thin film processes is adopted to enhance not only thin film characteristics but also the adhesion to underlying substrates. It is common practice to apply thermal energy for the improvement of the thin film characteristics and their heterogeneous bonding with the substrates [1-3]. However, due to the specifics of materials, the use of other forms of energy such as UV [4] or ion beam [5] becomes popular. Particularly, in the case of polymer substrates such as polyimide (PI), poly-ethylene-terephthalate (PET), and polycarbonate (PC), or ultra-thin glass substrates having a thickness of several hundreds of micrometers or less, ion beam process is adopted rather than thermal energy [6-10].

The ion beam energy is divided into two major categories depending on the acceleration state of the ions; 200 ~ several keV region which can cause surface damage such as etching and surface modification and a few keV ~ MeV region where ion implantation can occur. The ion beam-assisted modification of surface is used in various forms during the process of thin-film surface preparation or post-deposition process [11-13]. As an ion beam source, there are two sources used widely; an anode type ion beam source [14,15] and an RF type ion beam source [16] and both sources use gas injection inside the ion beam source block.

Recently, since the proportion of sputtering in industrial PVD (physical vapor deposition) is very high, it is urgently required to replace the thermal treatment process for the sputtering. However, the working pressure in the sputtering method is an important parameter for determining thin film characteristics. The sputtering generally operates stable in a region higher working pressure than the driving pressure of the ion beam source. Therefore, it is very important, in the same vacuum apparatus, to perform the sputtering and the ion beam treatment simultaneously and stably.

In this paper, we investigated plasma phenomena around the critical pressure of the ion beam sources driven by not only the charge repulsion mechanism but also the diffusion mechanism, respectively and studied the behavior of driving pressure of the ion beam source that it can be operated simultaneously with a sputtering process.

II. Experiments

For driving and characterizing the ion beam source, we employed a Plasma Complex Machining Center (PCMC™, Finesolution Co.) that was capable of plasma generation,

*Corresponding author
E-mail: yhuh@finesolution.co.kr, jeha@cju.ac.kr

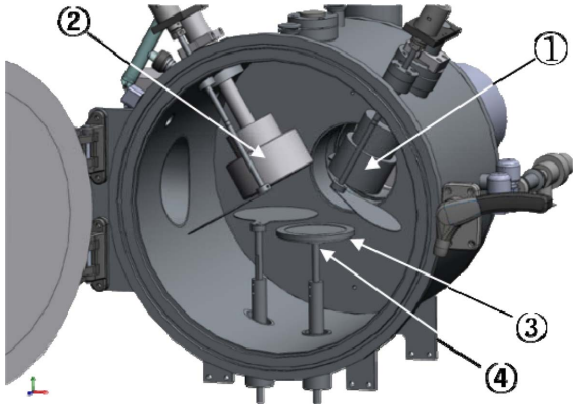

Figure 1. Configuration of a PCMC^{TM} vacuum chamber; ① anode plasma source, ② cathode plasma source, ③ Faraday sensor, ④ substrate holder.

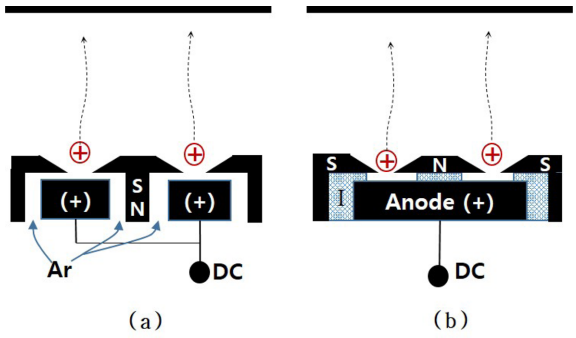

Figure 2. Design schematic of anode type ion beam source; (a) diffusion type, (b) charge repulsion type [20].

Figure 3. Ion beam shapes generated from an anode type ion beam source; (a) a normal beam shape, (b) an abnormal beam shape.

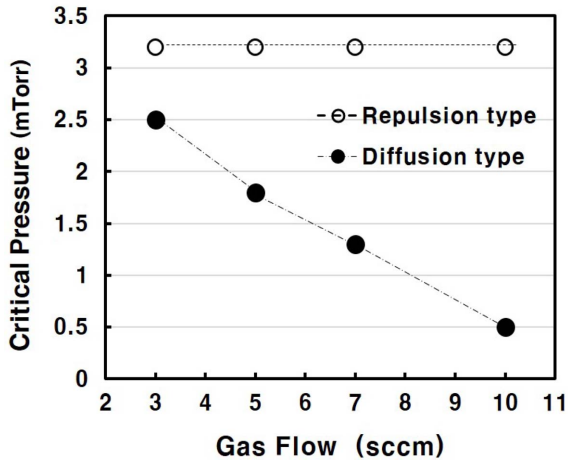

Figure 4. Critical pressure vs. Ar gas flow of the ion beam source; a diffusion type (●) and a charge repulsion type (○).

gas supply flow rate and pressure control. Figure 1 shows a schematic of PCMC^{TM}. There are two types of ion beam sources used for obtaining anode plasma in this experiment ; a diffusion type driven by injecting gas as in Fig. 2(a) and a charge repulsion type (FPG-C100S^{TM}, Finesolution Co.) without using injecting gas as in Fig. 2(b) [17-19].

The ion beam source was applied a voltage of 2,000 ~ 3,500 V for plasma generation and ion acceleration and was operated for 30~60 minutes. An argon (Ar) gas of high purity (5N) was used for plasma generation. An amount of injected gas was adjusted in the range of 3 to 10 sccm using a mass flow controller (MFC). The pressure of the vacuum chamber was measured using various ways; a Pirani gauge, a full range gauge (Pfeiffer), and a capacity diaphragm gauge (MKS). The surface of a glass substrate (45 mm × 45 mm × 0.7 mmt) was irradiated with an ion beam and characterized it using XPS (K-ALPHA, Thermo Fisher Scientific, UK). The temperature of the ion beam source was measured using thermal tape (THERMAX Lever 8, TMC Hallcrest Inc., UK).

III. Results and Discussion

Figure 3 is a typical photograph of (a) a normal ion beam shape of a collimation type and (b) an abnormal ion beam shape of a cotton type with a beam spread appearing in an anode type ion beam source. This phenomenon occurs in the anode type ion beam source regardless of the charge repulsion or diffusion mechanism. When the PCMC^{TM} reached the base pressure of typically ~5×10^{-6} Torr, the chamber pressure was gradually increased while keeping the argon gas injection amount constant at 5 sccm. In this case, the critical pressure (P_{crit}) is defined as the pressure at which the shape of the ion beam changes from the normal beam shape (Fig. 3(a)) to the abnormal beam shape (Fig. 3(b)).

The change in shape of the ion beam occurring below and above the critical pressure (P_{crit}) is described as follows. When the chamber pressure (P) becomes larger than P_{crit}, the mean free path (MFP) of the Ar gas becomes smaller so that the tunneling of the charge is generated. In this case, the generated (+) ions travels toward the magnetic pole surrounding the anode that is closest to the anode potential, instead of moving toward the anode potential [16]. Thus, the shape of ion beam is transformed around P_{crit}.

Figure 4 exhibits a graph of the critical pressures (P_{crit}) vs. Ar gas flow for the diffusion-type ion source (●) and the charge repulsion ion source (○), respectively. The voltage applied to the anode electrode was +3.5 kV. For the

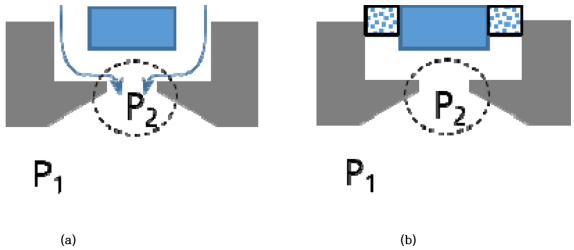

Figure 5. Schematic of driving model for (a) the diffusion type and (b) the charge repulsion type ion source.

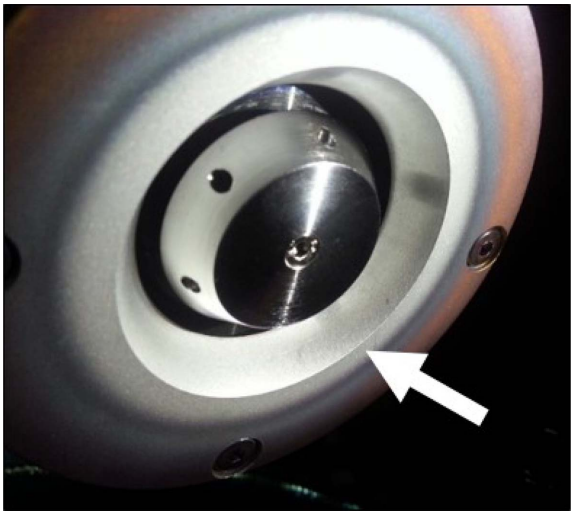

Figure 6. A picture of the front surface of ion beam source that was etched during an operation of the abnormal beam shaping at the condition of $P > P_{crit}$.

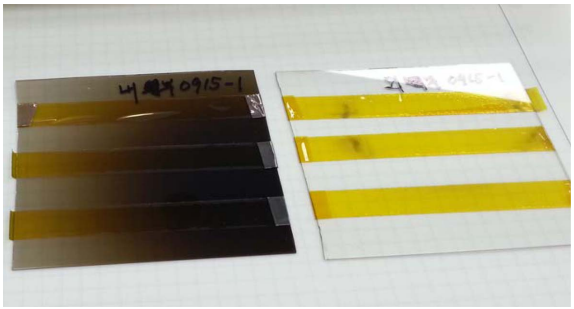

Figure 7. Glass surface treated with ion beam source; normal beam (right) and abnormal beam (left).

charge repulsion ion beam source, a normal ion beam shape was formed at $P < 3.2$ mTorr regardless of the gas injection rate. In contrast, for the diffusion type ion beam source the P_{crit} quasi-linearly decreased from 2.5 mTorr to 0.5 mTorr as the gas injection rate increased from 3 sccm to 10 sccm. As the gas injection increased, the critical pressure of the ion beam source was dropped linearly for the diffusion type while it remained at 3.2 mTorr for the charge repulsion type ion beam source. It is worth to point out that at the gas injection of 10 sccm, the range of having normal beam shape in the charge repulsion ion beam source is about 6.4 times wider than that in the diffusion type ion beam source.

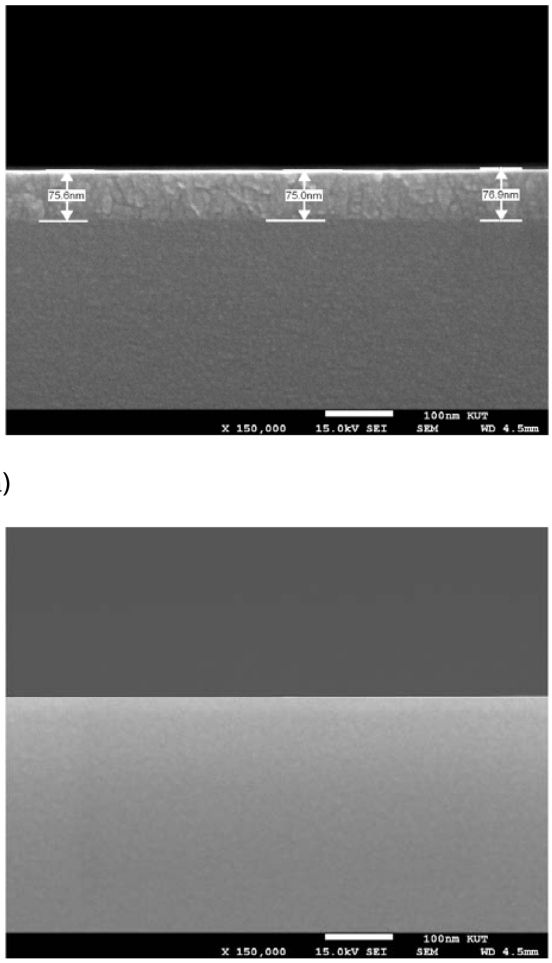

Figure 8. Cross-sectional SEM images of glass specimen treated by ion beam; (a) abnormal, (b) normal.

Figure 5 shows schematic of driving model for the ion beam shaping for the diffusion type and the charge repulsion type ion source. Figure 5(a) depicts the diffusion type ion beam source that generates a plasma by supplying the plasma ionized gas into the ion beam source. In this case, the Ar gas flow through the inside of ion beam source so that P_2 pressure becomes higher than P_1 pressure. Thus, the MFP of gas molecules at the P_2 point is relatively short and becomes shorter as the gas injection increases. In other words, when Ar gas flows the critical pressure in the diffusion type ion beam source is determined at a low value and is reduced more when the gas injection enlarges further.

Figure 5(b) shows the internal structure of the charge repulsion type ion beam source that generates plasma by using the gas existing outside the ion beam source. Since the gas is injected into the vacuum chamber not through the inside of the ion beam source like the diffusion type, P_1 and P_2 pressures become almost identical. And since no gas flows through the ion beam source, the pressures at P_1 and P_2 can always be maintained at similar values.

Therefore, the charge repulsion type ion beam source could have the same critical pressure even if the gas injection varied in the range of 3-10 sccm.

As described earlier, the diffusion type ion beam source has a narrower range of driving pressure for the normal beam shape. If the ion beam source is being operated in the in-situ process simultaneously with a sputtering apparatus, the critical phenomenon takes place easily even at a slight change of chamber pressure. Figure 6 is a picture of the front magnetic pole of the charge repulsion type ion beam source which maintained the abnormal beam state for 60 minutes. An etched trace looks similar to the target surface of the sputter cathode as directed by an arrow in Fig. 6.

Figure 7 is a photograph of glass specimen subjected to ion beam treatment using the charge repulsion type ion beam source. Both glass substrates were exposed to the ion beam for 60 minutes at the gas injection of 5 sccm below and above the critical pressure P_{crit}; normal (right) and abnormal (left).

Figure 7 shows the surface seriously contaminated when treated with the abnormal beam. Figure 7 (right) is the surface of the glass specimen treated with a normal beam at P = 2.8 mTorr and Fig. 7 (left) is the result formed with an abnormal beam at 3.6 mTorr. Figure 8 is cross-sectional SEM images of the glass specimen treated by ion beam for both (a) abnormal and (b) normal beam. As shown in the figure, the specimen treated with the abnormal ion beam was observed to have a thin film coated with impurities at a thickness of 75 nm.

Figure 9 is the XPS spectra measured to identify the surface components of the glass specimen displayed in Fig. 7. Figure 9(a) is the result measured from the reference specimen with no ion beam treatment, and (b) is the spectrum of the glass surface exposed to the abnormal beam. (c) is the spectrum of the glass surface treated with the normal beam. From (a) and (c), elements such as Si, Ca, Na, O and C were detected. As in the inside detail of (b), however, a peak of Fe 2p (KE = 776.68 eV) of 12.88 at. % was observed among three elements of O, Fe and C. It was analyzed that some elements etched from the magnetic poles around the anode were deposited on the glass substrate.

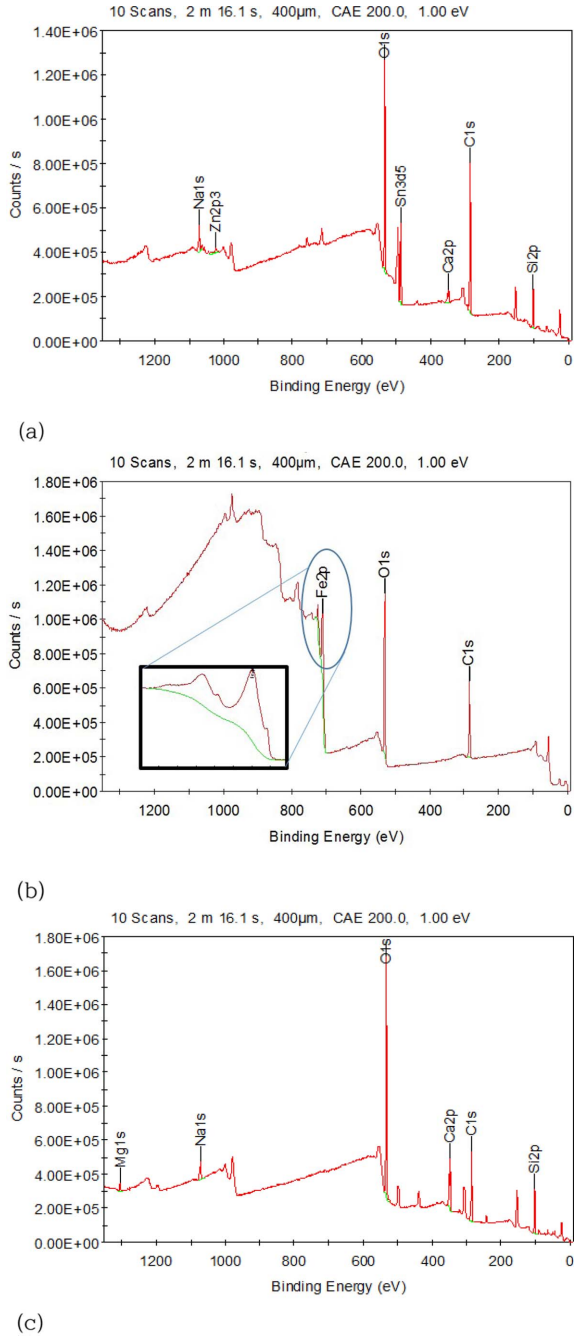

Figure 9. XPS spectra obtained from glass specimens; (a) a reference specimen, (b) abnormal beam treated, (c) normal beam treated.

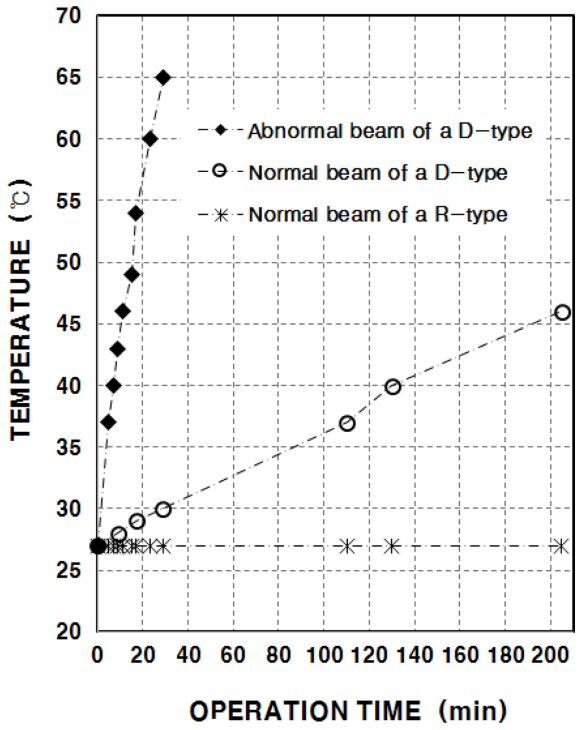

Figure 10. Temperature of ion beam sources vs. operation time; (1) diffusion type for normal beam (○) and abnormal beam (◆) and (2) charge repulsion type for normal beam (*).

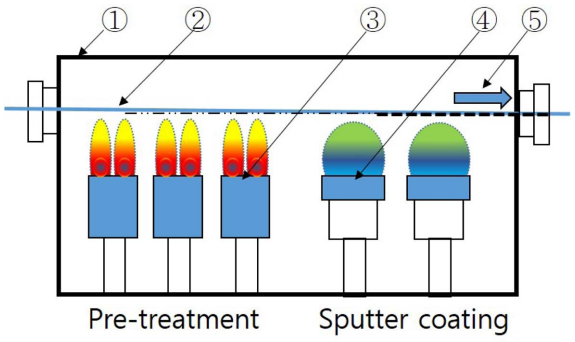

Figure 11. Schematic view of a roll-to-roll sputtering system driven at the same pressure as the ion beam source; ① vacuum chamber, ② web of film, ③ ion beam source, ④ sputter cathode, ⑤ outlet.

Figure 10 is the behavior of the body temperature by the ion beam source for a long period of operation time for the diffusion type for normal beam and abnormal beam and the charge repulsion type for normal beam. In the case of an abnormal beam, we observed that the body temperature of the diffusion type source (◆ symbol) increased rapidly at the rate of 1.9°C/min, which was the same for the charge repulsion type source (not shown).

Figure 11 shows an example of roll-to-roll surface treatment process prior to sputter coating in a thin film process that is typically used for substrates of either polymer or ultra-thin glass. The discharge of the ion beam source utilizes the 'Townsend regime' occurring in the 'dark discharge' region where the voltage is high and the ion current is very small. On the other hand, however, the discharge of the sputter cathode utilizes the 'glow discharge' phenomenon in which the voltage is low and the ion current is high. Due to such a significant difference in operating mechanism, it is very difficult to drive the sputter cathode and the anode type ion beam source simultaneously in the same vacuum environment. In the range of 1×10^{-3} to 5×10^{-2} Torr where sputter deposition process is being done it is very advantageous for surface treatment to employ an ion beam source with a charge repulsion type because of its good features with a normal beam of a wide range of the operating pressure, no impurity generation and no body heating [19] for a long period of operation.

IV. Conclusions

In this experiment, we investigated plasma phenomena around the critical pressure of the ion beam sources driven by not only the charge repulsion mechanism but the diffusion mechanism, respectively and studied the behavior of driving pressure of the ion beam source that it can be operated simultaneously with a sputtering process. The critical pressure P_{crit} of the diffusion type ion beam source was linearly decreased from 2.5 mTorr to 0.5 mTorr when the gas injection was varied in 3~10 sccm, while the P_{crit} of the charge repulsion ion beam source was remained at 3.5 mTorr. For $P < P_{crit}$, a collimated (normal) ion beam was formed while for $P > P_{crit}$ a cotton type (abnormal) ion beam was generated. At the gas injection of 10 sccm, the range of having normal beam shape in the charge repulsion ion beam source was about 6.4 times wider than that in the diffusion type ion beam source. When operates using an abnormal beam, an impurity of Fe 2p (KE = 776.68 eV) of 12.88 at. % was observed among three elements of O, Fe and C. The body temperature of the diffusion type ion beam source was observed to increase rapidly at the rate of 1.9°C/min and to vary at the rate of 0.1°C/min for an abnormal beam and normal beam, respectively. When used simultaneously with sputter deposition, it is very advantageous for surface treatment to employ an ion beam source with a charge repulsion type because of its good features with a normal beam of a wide range of the operating pressure, no impurity generation and no body heating for a long period of operation.

Acknowledgments

This research was a part of the project titled 'Characteristics of critical pressure for a beam shape of the anode type ion beam source' funded by the Ministry of Oceans and Fisheries, Korea.

References

[1] J. A. Thornton, J. Vac. Sci. Technol. 11, 666 (1974).
[2] K. Guenther, SPIE 1324, 2 (1990).
[3] B. Movchan and A. Demchishin, Fiz. Met. Metalloved 28, 653 (1969).
[4] Y. H. Ham, D. A. Shutov, K. H. Baek, L. M. Do, K. S. Kim, C. W. Lee, and K. H. Kwon, Thin Solid Films 518, 6378 (2010).
[5] S. K. Koh, S. C. Choi, S. Han, J. Cho, W. K. Choi, H.-J. Jung, and H. H. Hur, Key Eng. Materials 137, 107 (1998).
[6] D. R. Wheelers and S.V. Pepper, J. Vac. Sci. Technol. 20, 443 (1982).
[7] H. Schonhorn and R. H. Hansen, J. Appl. Polym. Sci. 11, 1461 (1967).
[8] S. Kim, J. Lee, and C. K. Hwangbo, J. Kor. Vac. Soc. 11, 141 (2002).
[9] S. Kim, J. Lee, and C. K. Hwangbo, Thin Solid Films 475, 155 (2005).
[10] J. Park, B. Park, S. Kang, K. K. Lee, D. Lee, and K. Lee, J. Kor. Inst. Surf. Eng. 41, 88 (2008).
[11] H. R. Kaufman and M. E. Harper, 2004 SPIE Proceeding, Vol. 5527 (2004).
[12] M. L. Fulton, SPIE 2253, 374 (2013).
[13] E. S. Cho and S. J. Kwon, J. Kor. Vac. Soc. 22, 26 (2013).
[14] H. W. Choi, D. H. Park, J. H. Kim, W. K Choi, Y. J. Sohn, B. S. Song, J. Cho, and Y. S. Kim, J. Kor. Vac. Soc. 16, 79 (2007).
[15] S. Lee and D.-G. Kim, Appl. Sci. Conv. Technol. 24, 162 (2015).
[16] E. S. Cho and S. J. Kwon, J. Kor. Vac. Soc. 22, 26 (2013).
[17] Finesolution, Patent No. KR10-1478216, Dec. 24 (2014).
[18] Finesolution, Patent No. US9,269,535 B1, Feb. 23 (2016).
[19] Y. Huh, Y. Hwang, and J. Kim, Appl. Sci. Conv. Technol. 27, 47 (2018).